Res Chem Intermed (2015) 41:881–897
DOI 10.1007/s11164-013-1240-y

Computer simulation of chemical reactions occurring in collapsing acoustical bubble: dependence of free radicals production on operational conditions

Slimane Merouani · Oualid Hamdaoui · Yacine Rezgui · Miloud Guemini

Received: 18 February 2013 / Accepted: 25 April 2013 / Published online: 10 May 2013
© Springer Science+Business Media Dordrecht 2013

Abstract Acoustic cavitation is responsible for both sonochemistry and sonoluminescence. In this theoretical investigation, computer simulation of chemical reactions occurring in an isolated cavitation bubble oscillating in water irradiated by an ultrasonic wave has been performed for various acoustic amplitudes, different static pressures and diverse liquid temperatures to study the relationship between these three key parameters in sonochemistry and the oxidants created in the bubble. The results of the numerical simulations indicated that the main oxidants created in an O_2 bubble are $^{\bullet}OH$ radical and O atom. The amount of the oxidants formed in the bubble at the end of the bubble collapse increases as the acoustic amplitude increases from 1.5 to 3 atm. For each acoustic amplitude, there exists an optimal static pressure for the production of the oxidants, which shifts toward a higher value as the acoustic amplitude increases. Correspondingly, for each acoustic amplitude, an optimum of liquid temperature was observed at 20 °C for $^{\bullet}OH$, $HO_2^{\bullet}$ and H_2O_2. The simple model adopted in this work, after comparisons with the trends obtained with the literature experimental observations, seems to satisfactorily explain the experimental observations and should practically aid in optimization of operating conditions for sonochemical reactions. Results from this study were discussed and some recommendations were given.

Keywords Sonochemistry · Computer simulation · Chemical reactions · Acoustic amplitude · Static pressure · Liquid temperature

S. Merouani · O. Hamdaoui (✉)
Laboratory of Environmental Engineering, Department of Process Engineering, Faculty of Engineering, Badji Mokhtar—Annaba University, P.O. Box 12, 23000 Annaba, Algeria
e-mail: ohamdaoui@yahoo.fr; oualid.hamdaoui@univ-annaba.org

Y. Rezgui · M. Guemini
Laboratory of Applied Chemistry and Materials Technology, University of Oum El-Bouaghi, P.O. Box 358, 04000 Oum El Bouaghi, Algeria

Introduction

Chemical effects of ultrasound (sonochemistry) are due to the phenomenon of acoustic cavitation, which involves the formation and the subsequent collapse of microbubbles from acoustical wave-induced compression/rarefaction [1]. The microbubbles formed during the rarefaction part of the wave contain vaporized liquid or gas, which was previously dissolved in the liquid. The microbubbles can be either stable, oscillating about their average or equilibrium size for many acoustic cycles, or transient when they grow to a certain size in one or at most a few acoustic cycles and violently collapse during the compression part of the wave [2]. The sudden collapse of these microbubbles leads to localized, transient high temperatures and pressures (up to and above 5,000 K and 1,000 atm, respectively [1, 3]), resulting in the generation of highly reactive species including hydroxyl ($^{\bullet}OH$), hydrogen ($H^{\bullet}$) and perhydroxyl ($HO_2^{\bullet}$) radicals and hydrogen peroxide (H_2O_2) [3, 4]. The formation of $H^{\bullet}$ and $^{\bullet}OH$ is attributed to the thermal dissociation of water vapor present in the cavities during the compression phase [3, 4]. The radicals generated either react with each other to form new molecules and radicals or diffuse into the bulk solution to serve as oxidants [4]. Reactions involving free radicals can occur within the collapsing bubble, at the interface of the bubble and in the surrounding liquid [3–5]. Under certain conditions, bubble collapse can also result in light emission, sonoluminescence, originating from the core of the bubble during the final stages of collapse [6].

Several recent studies have attempted to explain the interactions between bubble dynamics and chemical reactions occurring in the bubble. For example, Kamath et al. [7] estimated the production of $^{\bullet}OH$ radicals by decoupling the bubble dynamics equation and the chemical kinetics. Prasad Naidu et al. [8] modeled the equilibrium production of various radicals using the Rayleigh–Plesset equation for the radial motion of the bubble, coupled with Flynn's assumption that the bubble becomes a closed system during collapse, when the partial pressure of gas becomes equal to the vapor pressure. The entire growth period and the initial phase of the collapse were assumed to be isothermal, whereas the later stage of the collapse was considered to be adiabatic. Gong and Hard [9] also adopted a similar approach of coupling bubble dynamics with the chemical kinetics and explained some trends in sonochemistry. Other complex models that adopt the combination approach were also available in the literature [10–12].

Several experimental studies on the influence of operating parameters such as acoustic amplitude, static pressure and liquid temperature on sonochemistry and/or sonoluminescence have been published and have shown the importance of these parameters. In the present paper, we focused our study on the basis of the hot spot theory [13] to investigate theoretically the effects of acoustic amplitude, static pressure and liquid temperature on sonochemical production of oxidizing species in collapsing bubble using a model that combines the dynamic of bubble collapse with the chemical kinetics of single cavitation bubble. Chemical reactions occurring in an isolated bubble oscillating in water irradiated by an ultrasonic wave were simulated for various acoustic amplitudes (up to 3 atm), different static pressures (0.2–3 atm) and diverse liquid temperatures (10–60 °C). Results from this model are used to explain some experimentally observed sonochemical phenomena.

Model

Bubble dynamics model

A gas and vapor filled spherical bubble isolated in an infinite, compressible and viscous liquid oscillates under the action of a sinusoidal sound wave. The temperature and pressure in the bubble are assumed to be spatially uniform and the gas content of the bubble behaves as an ideal gas [14]. The radial dynamics of the bubble is described by a good model furnished by the Keller–Miksis equation [15, 16]:

$$\left(1-\frac{\dot{R}}{c}\right)R\ddot{R}+\frac{3}{2}\left(1-\frac{\dot{R}}{3c}\right)\dot{R}^2=\frac{1}{\rho_L}\left(1+\frac{\dot{R}}{c}+\frac{R}{c}\frac{d}{dt}\right)[p_B-P(t)] \tag{1}$$

in this equation dots denote time derivatives (d/dt), c is the speed of sound in the liquid, ρ_L is the density of the liquid, $P(t)$ denotes the sum of the static ambient pressure and the time-dependent pressure field driving the bubble into oscillation and p_B is the pressure on the liquid side of the interface, related to the bubble internal pressure p by the balance of normal stresses across the interface, namely:

$$p_B=p-\frac{2\sigma}{R}-4\mu\frac{\dot{R}}{R} \tag{2}$$

in which σ is the surface tension and μ is the liquid viscosity.

In the present study, we consider ambient pressures of the form [16]:

$$P(t)=p_\infty-P_\mathrm{A}\sin(2\pi ft) \tag{3}$$

where p_∞ is the static pressure, P_A is the acoustic pressure amplitude and f is the sound frequency. The acoustic amplitude P_A is correlated with the acoustic intensity I_a, or power per unit area, as $P_\mathrm{A}=(2I_\mathrm{a}\rho_L c)^{1/2}$ [3]. Equation (1) is only accurate to first order in the bubble wall Mach number ($\dot{R}/c$) but, for all acoustic amplitudes in this study, this level of accuracy is sufficient (the speed of the bubble wall ($|\dot{R}|$) at the collapse never exceeds the sound velocity in the liquid (c), which is the assumption used in the derivation of the equation) [15].

In the present model, the expansion of the bubble is considered as isothermal and its total compression (implosion phase) is treated as adiabatic [11, 17]. The mass and heat transfer at the bubble wall have not been considered in this study and it should be noted that there exist some research studies that include these effects [9–12, 18]. For a comparative point of view, the inclusion of these effects, leading to a realistic situation, might change the absolute values of the predicted collapse temperature and pressure but definitively will not change the predicted trends, including the quantitative variation of the maximum radius, the collapse time and the maximum collapse temperature with variation in operational conditions [11, 18]. Additionally, the importance of mass and heat transfer occur over multiple cycles of oscillation changing, in this case, the internal composition of the vapor phase [9]. Consequently, as the present numerical calculations were carried out for one acoustic cycle, the mass and heat transfer will not also affect significantly the

quantitative bubble yield, predicted in one acoustic cycle. So, in order to reduce computational parameters, the current model takes, as input, initial bubble vapor content and neglects mass and heat transfer during bubble expansion and collapse.

On the basis of the above assumptions, the pressure and temperature inside the bubble at any instant during adiabatic phase can be calculated from the bubble size, using the adiabatic law:

$$p = \left[P_{\mathrm{v}} + P_{g0}\left(\frac{R_0}{R_{\max}}\right)^3\right]\left(\frac{R_{\max}}{R}\right)^{3\gamma} \tag{4}$$

$$T = T_{\infty}\left(\frac{R_{\max}}{R}\right)^{3(\gamma-1)} \tag{5}$$

where P_v is the vapor pressure, $P_{g0} = p_{\infty} + (2\sigma/R_0) - P_v$ is the gas pressure in the bubble at its ambient state ($R = R_0$), R_0 is the ambient bubble radius, T_{∞} is the bulk liquid temperature, $R_{\max}$ is the maximum radius of the bubble and γ is the ratio of specific heats capacities (c_p/c_v) of the vapor/gas mixture. It is important to notice here that the assumption of spatial uniform pressure and temperature inside the bubble is valid as long as inertia effects are negligible and the velocity of the bubble wall is below the speed of sound in the vapor/gas mixture. This assumption was justified in detail in the paper published by Kamath et al. [9]. Also, Yasui et al. [10] and Fujikawa and Akamatzu [19] were pointed out in their models which include heat transfer that the bubble temperature and pressure are roughly uniform except at a very thin layer, called thermal boundary, near the bubble wall.

Several physical properties in the above equations change with the liquid temperature (water is the liquid medium in this study). They have estimated as follows:

- *Vapor pressure*: The vapor pressure of water P_{v}(in N m^{-2}) at temperature T (in K) is calculated using Antoine's equation [20]:

$$\ln(P_{\mathrm{v}}/133.32) = 18.3036 - \frac{3816.44}{T - 46.13} \tag{6}$$

- *Liquid density*: The density of water ρ_{L} (in kg m^{-3}) at any temperature T (in °C) is estimated by the following correlation [21]:

$$\rho_{\mathrm{L}} = 334.71 \times 0.274^{\left(1-\frac{T}{T_{\mathrm{C}}}\right)^{2/7}} \tag{7}$$

where T_{c} is the critical temperature of water (374.2 °C).

- *Surface tension*: The surface tension of water σ (in N m^{-1}) is estimated as function of temperature (in K) by the following expression [22]:

$$\sigma = 0.2358\left(\frac{647.15 - T}{647.15}\right)^{1.256} \times \left[1 - 0.625\left(\frac{647.15 - T}{647.15}\right)\right] \tag{8}$$

- *Liquid viscosity*: The viscosity of water μ (in N m^{-2} s) is calculated as function of temperature T (in K) in the range of 273–373 K by [23]:

$$\mu = 10^{-3} \times \frac{(T-27)}{[0.05594(T-273)+5.2842](T-273)+137.37} \tag{9}$$

- *Speed of sound*: The speed of sound c (in m s^{-1}) was correlated as function of temperature T (in K) in the range 273–373 K by the following interpolated polygon obtained by interpolation of the *International Steam Tables* experimental data [24]:

$$c = 1402.7 + 4.9045(T-273) - 4.72\times10^{-2}(T-273)^2 + 1.242\times10^{-4}(T-273)^3 \tag{10}$$

We would like to mention here that experimental data [24, 25] shows that the elevation of ambient static pressure in the range of 0.2–3 atm has no effect on physical properties of water.

In the present model, the maximum internal temperature and pressure reached in the bubble at the end of the bubble collapse are approximated by:

$$T_{\max} = T_{\infty}\left(\frac{R_{\max}}{R_{\min}}\right)^{3(\gamma-1)} \tag{11}$$

$$p_{\max} = \left[P_{\mathrm{v}} + P_{g0}\left(\frac{R_0}{R_{\max}}\right)^3\right]\left(\frac{R_{\max}}{R_{\min}}\right)^{3\gamma} \tag{12}$$

where $R_{\min}$ is the minimum radius of the bubble at the collapse (corresponded to the velocity of the collapse *dR/dt* equal to zero).

Chemical kinetics model

For a bubble initially containing oxygen and water vapor, a kinetic mechanism consisting in nineteen elementary chemical reactions is taken into account involving the chemical species O_2, H_2O, $^{\bullet}OH$, $H^{\bullet}$, O, $HO_2^{\bullet}$, H_2 and H_2O_2. The kinetic mechanism used in the present numerical simulations was detailed in the literature [7, 26, 27].

The chemical kinetics model consists of the reaction mechanism and determines the production as function of time of each species during the bubble collapse. The detail of the chemical model used for the simulation of the reactions system has been well described by Choi et al. [28].

Procedure of the numerical simulation

The simulation of the reactions system occurring in the bubble starts at the beginning of the adiabatic phase (at time corresponded to $R_{\max}$). The input parameters of the reactions system are the composition of the bubble on water vapor and oxygen at this point, the temperature and pressure profiles in the bubble during adiabatic phase and the collapse time. All these parameters were obtained by solving the dynamics equation (Eq. 1). The bubble temperature increases during the adiabatic phase, the reaction system evolves and radicals start to form by thermal

dissociation of H_2O and O_2 molecules in the bubble. Thus, the composition of the bubble on all species expected to be present (O_2, H_2O, $^{\bullet}OH$, $H^{\bullet}$, O, $HO_2^{\bullet}$, H_2 and H_2O_2) was determined at any temperature during the collapse phase. The simulation of the reactions system was stopped after the end of the bubble collapse. The numerical simulation performed for all conditions indicated that the amount of each chemical species created inside a bubble attained their upper limit at the end of the collapse as the bubble temperature and pressure reached their upper values at this point. Thus, in the following, the amount of each species created in the bubble is defined as that of the end of the bubble collapse. Also, the sonochemical activity of a bubble is represented by the amount of the oxidants, which is defined as the sum of the number of moles of all the oxidants ($^{\bullet}OH$, $HO_2^{\bullet}$, $H^{\bullet}$, O, H_2O_2) formed in the bubble per collapse.

It is important to mention here that a lot of numerical reports that do not insert the kinetics part in their studies interpret the overall efficiency of sonochemical reactions, i.e. radical production, on the basis of just many output results of single-bubble dynamics (example: maximum temperature or pressure, collapse time or R_{max}/t_c where t_c is the collapse time). These interpretations are not really justified because the single-bubble sonochemical yield, i.e. free radicals production, results from the interaction of all the output results of the bubble dynamics, which are declared in the current study as inputs for the chemical kinetics model. Because of this, the kinetic results provided by the present numerical simulations should be a very justified starting point for interpreting the overall qualitative sonochemical observations.

Results and discussion

The range of ultrasound frequency commonly used in sonochemistry is from 20 kHz to $\sim$1 MHz. However, in recent research, an optimum ultrasonic frequency has been reported to be around 300 kHz with regard to the rate of H_2O_2 production and pollutants oxidation [29–31]. Thus, the present numerical simulations have been performed at 300 kHz.

Effect of acoustic amplitude

Numerical simulations of chemical reactions occurring in an O_2 bubble oscillating under the ultrasound frequency of 300 kHz have been performed for various acoustic amplitudes (up to 3 atm). The static pressure is 1 atm and the liquid temperature is 20 °C. According to some recent experimental studies [32–34], the ambient radius (R_0) of a typical active bubble is strongly dependent on the acoustic amplitude, and results from these studies showed that R_0 increases as acoustic amplitude increases. In our recent paper [35], we have studied in detail the effects of acoustic amplitude and ultrasonic frequency on the ambient radius (R_0) for an isolated cavitation bubble. Results from the study agree well, qualitatively and quantitatively, with the experimental observations as illustrated in this paper [35]. Thus, in the present numerical simulations, the ambient radius (R_0) was selected as function of acoustic amplitude according to our previous study [35] as 3.5 μm for

1.5 atm, 4.25 μm for 2 atm, 5.25 μm for 2.5 atm and 6 μm for 3 atm. To the best of our knowledge, this approach of varying initial bubble radius (R_0) with acoustic amplitude has rarely been addressed before in the existing numerical calculations.

In Fig. 1, the amount of each chemical oxidant created in the bubble per collapse is shown as function of acoustic amplitude. The obtained results clearly demonstrate that an increase in acoustic amplitude from 1.5 to 3 atm results in an intense increase in the amount of the oxidants.

While the present model focuses on single bubble, experimental results reported in the literature were obtained from a bulk solution (multibubble system). Therefore, an exact comparison between this model and experimental results is impossible. This is in fact due to the complexity of the multibubble system which includes the bubble–bubble interactions phenomenon (coalescence, clustering, etc.) that is not considered in the present model. However, bearing in mind all the considerations, it clearly appears that the trends of the sonochemical yields in single bubble (Fig. 1) are consistent with that in bulk solutions observed in various reports on the effect of acoustic amplitude on the sonochemistry reaction yield. For example, Koda et al. [31] analyzed the variation in the sonochemical efficiency in various laboratory-scale sonochemical reactors of operating power in the range of 35–220 W with irradiation frequency in the range of 25–1,200 kHz. The obtained results indicate that sonochemical efficiency as quantified by chemical dosimetry increases linearly with increasing ultrasonic power. In our previous work [36], we found at 300 kHz that sonochemical production of I_3^-, Fe^{3+} and H_2O_2 increased with increasing acoustic power from 13.7 to 25.7 W. At 300 kHz, Mark et al. [37] measured sonochemical yields of the $^{\bullet}OH$ radicals as a function of the acoustic power input.

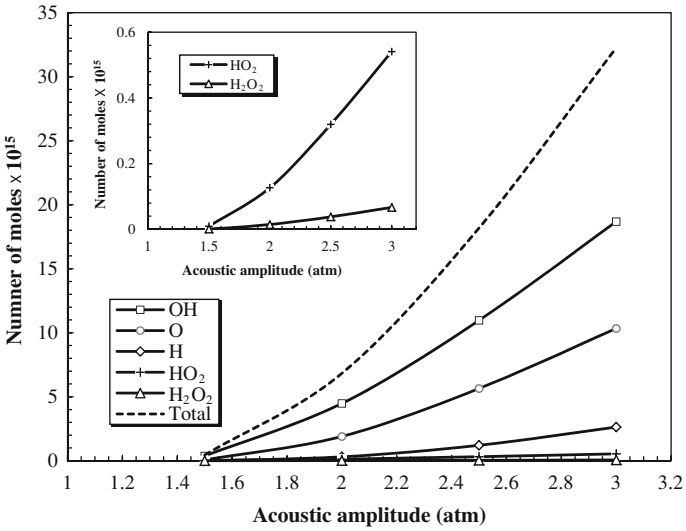

Fig. 1 Production per collapse of each chemical oxidant created in the bubble as function of acoustic amplitude. The lateral figure is a zoomed view for HO_2 and H_2O_2 (conditions: ambient bubble radius: 3.5 μm for 1.5 atm, 4.25 μm for 2 atm, 5.25 μm for 2.5 atm and 6 μm for 3 atm; frequency: 300 kHz; liquid temperature: 20 °C; static pressure: 1 atm)

They found that the yield of the •OH increased with the increase of acoustic power up to a plateau. Kanthale et al. [38] showed that the H_2O_2 yields and sonoluminescence intensities in water increase with acoustic power (2–20 W) for all the tested irradiation frequencies (213, 355, 647, and 1,056 kHz).

The increase in the predicted single-bubble sonochemical yields with acoustic amplitude may be explained as follows: with an increase in acoustic amplitude, the expansion ratio of the cavity (R_{max}/R_0) will increase and, since the partial pressure of water is always equal to vapor pressure, more water vapor should be present inside the cavity to cushion the collapse. But, in turn, the compression ratio of cavity (R_{max}/R_{min}) also increases with increasing acoustic amplitude, leading to increase the collapse temperature as indicated in Fig. 2. In addition, the increase in the amount of the trapped water with increasing acoustic amplitude (Fig. 2) can promote the formation of free radicals, since they result from the dissociation of the water molecules. Consequently, an increase in acoustic amplitude will thus result in greater sonochemical effects in the collapsing bubble.

As a recommendation for this operating parameter, the acoustic amplitude for 300 kHz sonochemistry processes should be selected, with great confidence, as high as possible in the range of 1.5–3 atm to ensure the maximum sonochemical activity. This is confirmed in the experiments of Torres et al. [39] conducted for the same conditions as the present numerical investigation.

Effect of static pressure

In order to study the static pressure dependence on the production of the oxidants, computer simulations have been performed for various static pressures (0.2–3 atm) and various acoustic amplitudes.

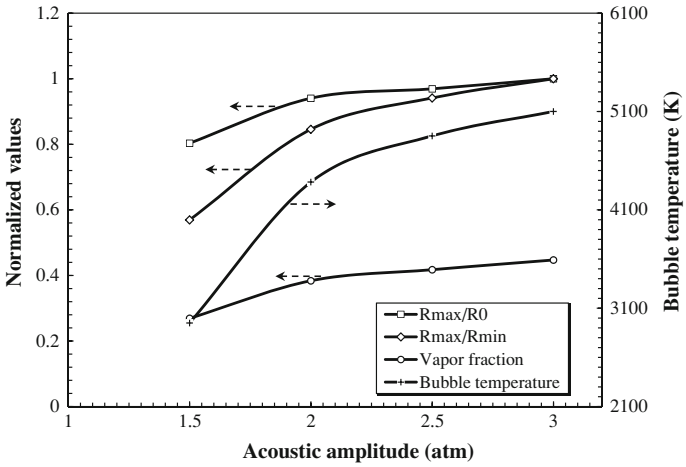

Fig. 2 Normalized expansion and compression ratios, trapped vapor fraction and bubble temperature as a function of acoustic amplitude. Results obtained for the same conditions as in Fig. 1. Values of expansion and compression ratios are normalized with respect to the corresponding maximum values obtained at 3 atm of acoustic amplitude

In Fig. 3, the amount of each oxidant created in the bubble per collapse is shown as a function of static pressure for 300 kHz and 2.5 atm of ultrasound frequency and acoustic amplitude, respectively. It is seen that the production of each oxidant occurs at a maximum rate at about 0.9 atm; at lower and higher static pressures, the effect decreases and finally reaches the threshold limit of the production, which is assumed as 10^{-22} mol [35], at 0.1 atm (the lower bound) and 3 atm (the upper bound). The observed maxima in the production of the oxidants at 0.9 atm of static pressure may be explained as a consequence of competing effects: the amount of water vapor trapped at the collapse and the expansion ratio of the bubble. These two parameters are presented together with the bubble temperature in Fig. 4. On the one hand, as the static pressure above the liquid increases, the amount of water vapor trapped in the bubble decreases, leading to higher specific heat ratio γ of the gas mixture (γ of water vapor, 1.33, is less than γ of oxygen, 1.4). Thus, the bubble temperature increases as γ increases. On the other hand, as the static pressure increases, the expansion ratio of the bubble decreases, resulting in a less violent collapse which reduces the bubble temperature. These two opposite effects should lead to an optimal bubble temperature and, thus, to maxima in the production rate of the oxidants. It is noted, therefore, that the increase of the static pressure works as if the acoustic amplitude decreases because the vapor content decreases and the bubble expands less.

In Fig. 5a, b, the calculated results as function of ambient static pressures are shown for various acoustic amplitudes. In Fig. 5a, the bubble temperature at the collapse is shown. It is seen that, for given acoustic amplitude, the bubble temperature initially increases with ambient static pressure, passes through a

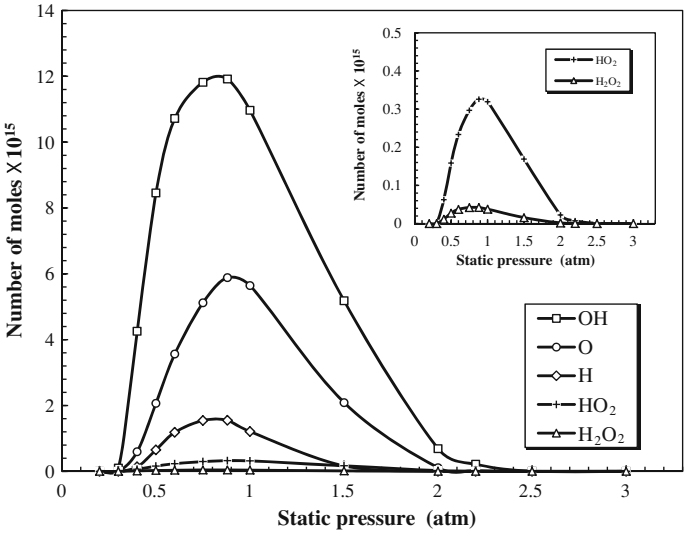

Fig. 3 Production per collapse of each chemical oxidant created in the bubble as function of static pressure. The *inset* is a zoomed view for HO_2 and H_2O_2 (conditions: ambient bubble radius: 5.25 μm; frequency: 300 kHz; acoustic amplitude: 2.5 atm; liquid temperature: 20 °C)

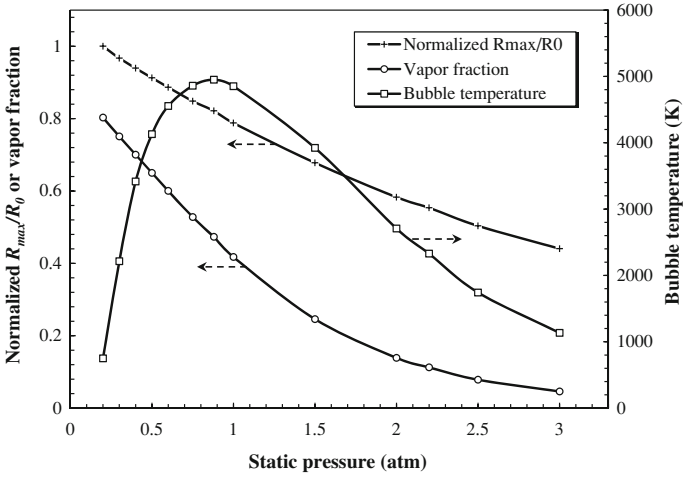

Fig. 4 Normalized expansion ratio, trapped vapor fraction and bubble temperature as function of static pressure. Results obtained for the same conditions as in Fig. 3. Values of expansion ratio are normalized with respect to the maximum value obtained at 0.2 atm of static pressure

maximum, and then decreases with the further increase in the static pressure. As the acoustic amplitude increases, the bubble temperature increases and the curve shifts toward a higher value of the static pressure. A similar behavior is observed for the amount of the oxidants created per collapse as a function of static pressure for various acoustic amplitudes as shown in Fig. 5b. From this figure, it is also observed that the lower and upper bounds of static pressure for the production of the oxidants increase with increasing acoustic amplitude. At the acoustic amplitude of 3 atm, the optimal static pressure for the production of the oxidants is 1 atm. This optimal value of the static pressure decreases to 0.9, 0.6, and 0.5 atm as the acoustic amplitude decreases, respectively, to 2.5, 2, and 1.5 atm (Fig. 5b). In addition, the amount of the oxidants created per collapse at the optimal static pressure decreases as the acoustic amplitude decreases.

Though an exact comparison between the predicted results (numerical simulations) in single-bubble and those in bulk solution (experiments) is not possible, the observed trend of the dependence of the production of the oxidants on static pressure agrees well with the experimental results. For example, the amount of hydrogen peroxide, nitrate and nitrite produced by ultrasound irradiation of water was found to be zero at air pressures less than 100 mm, above which it increases to maximum at 1,520 mm, finally decreasing to zero at 4,180 mm [40]. Similar results were reported by measurement of sonoluminescence intensity, but the maximum intensity of luminescence shifts toward higher static pressures when the ultrasonic power is increased [40], which is the same trend observed in Fig. 5a, because luminescence intensity depends on the maximum temperature of the collapse [40]. Henglein and Gutierrez [41] found at 1 MHz that, as the static pressure increases, the rate of KI oxidation increases to a maximum and then decreases with a

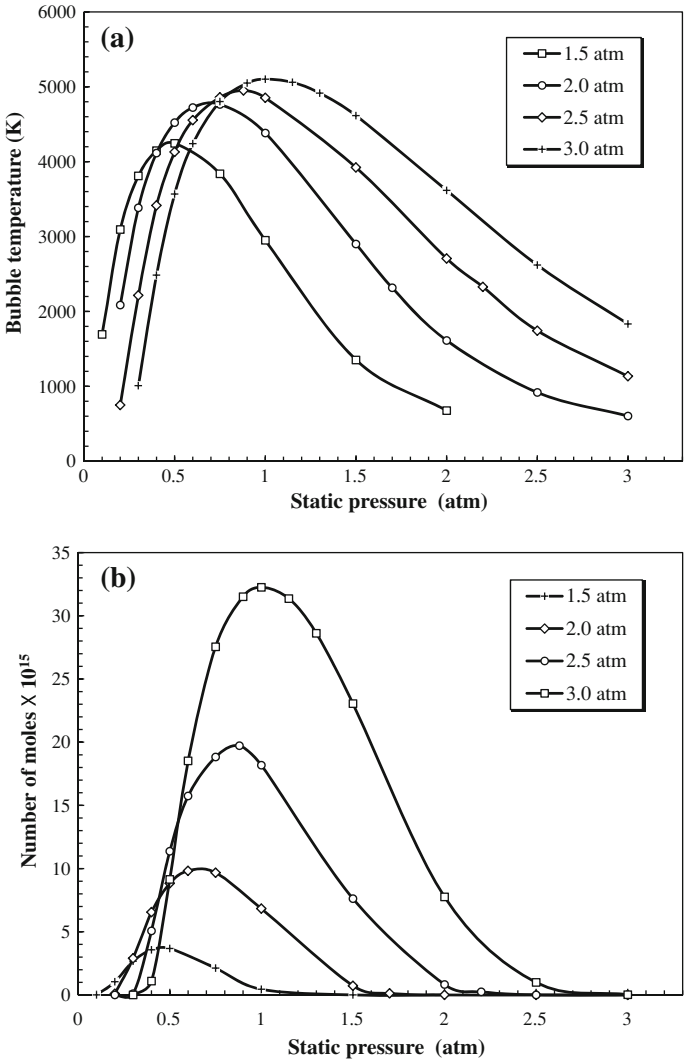

Fig. 5 **a** Bubble temperature and **b** amount of the oxidants created in an O_2 bubble as function of static pressure for various acoustic amplitudes (conditions: ambient bubble radius: 3.5 μm for 1.5 atm, 4.25 μm for 2 atm, 5.25 μm for 2.5 atm and 6 μm for 3 atm; frequency: 300 kHz; liquid temperature: 20 °C)

continuous increase in static pressure. The maximum also shifts toward higher values of static pressure as the acoustic amplitude increases. Van Iersel et al. [42] found at 20 kHz that the sonochemical oxidation of iodide is increased with increasing static pressure from 1 to 5 bar and then decreases to zero at around 8 bar.

Basing on the results of the numerical simulations, we recommend to carrying out all experimental sonochemical reactions at 300 kHz of ultrasound frequency at atmospheric static pressure ($\sim$1 atm) for high acoustic amplitudes.

Effect of liquid temperature

Numerical simulations of chemical reactions inside an O_2 bubble have been performed for various liquid temperatures (10–60 °C) and diverse acoustic amplitudes (1.5–3 atm).

In Fig. 6, the amount of each oxidant created in the bubble per collapse is shown as a function of liquid temperature for the ultrasonic frequency of 300 kHz and the acoustic amplitude of 2.5 atm. It can be seen that the production of $^{\bullet}OH$, $HO_2^{\bullet}$ and H_2O_2 increases as the liquid temperature increases from 10 to 20 °C and then decreases with the further increase in the liquid temperature. For O and $H^{\bullet}$, there is no optimum. The production of O atoms decreases sharply with the increase of the liquid temperature. For $H^{\bullet}$, the production starts with a plateau at low temperatures and then decreases with an increase in the liquid temperature.

Numerical calculations of the bubble dynamics performed for liquid temperature ranging from 10 to 60 °C showed that liquid temperature has practically no effect on the expansion ratio and the collapse time of the bubble. Thus, the optima of $^{\bullet}OH$, $HO_2^{\bullet}$ and H_2O_2 can be explained as follows [12]: as the liquid temperature increases, the vapor pressure increases, and consequently more vapor is trapped by the collapse as can be seen in Fig. 7. This can promote the formation of free radicals since they come from the dissociation of the water molecules. But increasing the liquid temperature simultaneously involves less violent collapses (decreasing γ of the gas mixture) leading to a lower internal temperature at the end of the bubble collapse (Fig. 7), which reduces the decomposition of molecules into free radicals.

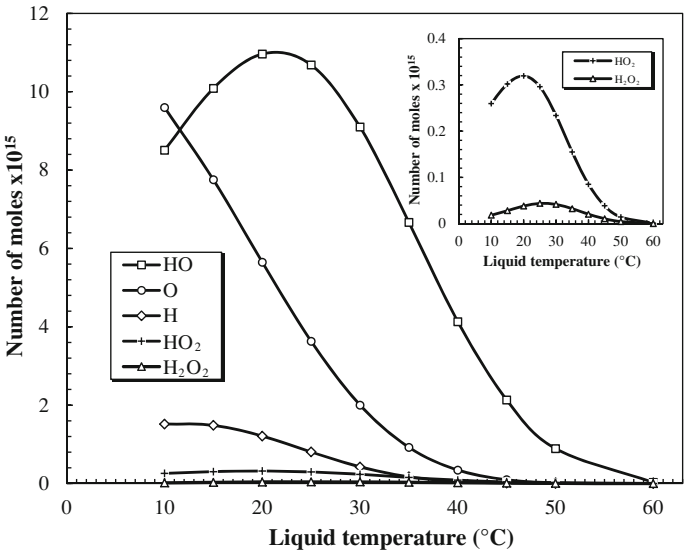

Fig. 6 Production per collapse of each chemical oxidant created in the bubble as function of liquid temperature. The *inset* is a zoomed view for HO_2 and H_2O_2 (conditions: ambient bubble radius: 5.25 μm; frequency: 300 kHz; acoustic amplitude: 2.5 atm; static pressure: 1 atm)

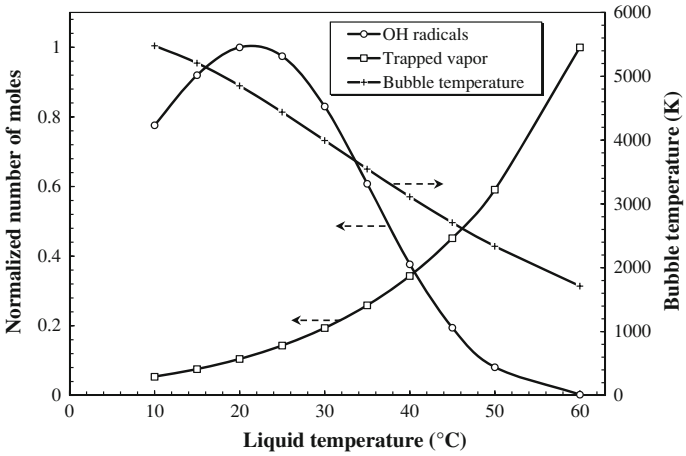

Fig. 7 Amount of water vapor trapped at the collapse, bubble temperature and amount of OH radical created in the bubble as function of liquid temperature. Results obtained for the same conditions as in Fig. 6

These two competing effects should lead to an optimum of the liquid temperature for the oxidants ($^{\bullet}OH$, $HO_2^{\bullet}$ and H_2O_2) formation as shown in Fig. 6.

In Fig. 8a, b, the bubble temperature and the amount of the oxidants created in the bubble per collapse, respectively, are shown as function of liquid temperature for various acoustic amplitudes. Figure 8a shows that, for given acoustic amplitude, the bubble temperature decreases monotonically as the liquid temperature increases. For 1.5 and 2 atm, the amount of the oxidants presents a maximum at 20 °C. However, at 2.5 and 3 atm, there is no optimum, but the amount of the oxidants starts with a slight plateau at low temperatures (less than 15 °C) and then decreases sharply with the further increase in liquid temperature above 15 °C. It seems that the optima of the liquid temperature shifts toward low temperature for high levels of acoustic amplitude. An exactly similar behavior has been reported by Entezari and Kruus [43] at 900 kHz for various acoustic powers (7, 25 and 76 W) when they examined the oxidation of potassium iodide in aqueous solutions.

Most observations reported in the literature concerning sonochemistry appear to indicate that an increase in the ambient liquid temperature results in an overall decrease in the sonochemical effect, which is what we obtained in our study (single-bubble system) at higher acoustic amplitudes (Fig. 8b). At 300 kHz, we have reported in our previous work [36] that the sonochemical degradation of iodide decreased with increasing temperature from 25 to 55 °C. Mark et al. [37] observed a monotonic decrease in $^{\bullet}OH$ and H_2O_2 yields in water as the liquid temperature increased. Using the terephtalate dosimetry, Mason et al. [44] and Iida et al. [45] found that, with sonication at higher temperature, there is a decrease in the fluorescence emission. At 20 kHz, the liberated triiodide decreased with increasing liquid temperature in the range 5–50 °C [43].

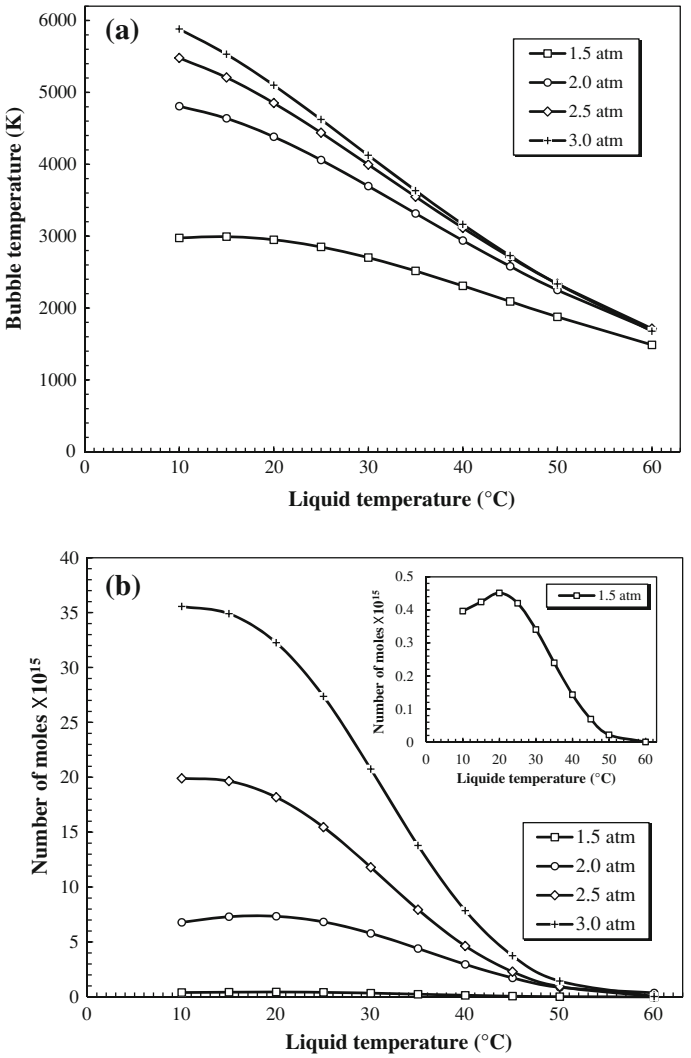

Fig. 8 **a** Bubble temperature and **b** amount of the oxidants created in an O_2 bubble as function of liquid temperature for various acoustic amplitudes. The *inset* in (**b**) is a zoomed view for 1.5 atm (conditions: ambient bubble radius: 3.5 μm for 1.5 atm, 4.25 μm for 2 atm, 5.25 μm for 2.5 atm and 6 μm for 3 atm; frequency: 300 kHz; static pressure: 1 atm)

Combining the above theoretical and experimental observations, to ensure maximum yields, sonochemical processes should be carried out at relatively low liquid temperatures (10–20 °C).

Finally, we would like to mention here that the overall efficiency of sonochemical reactions cannot be attributed to the single-bubble event alone but also to the number of active cavities formed in the reactor and to the bubble–bubble interaction phenomena (coalescence, clustering, etc.), which in turn depend on the

operational conditions of the experiment. For example, increasing acoustic amplitude will result, in addition to the rise of individual cavitation activity, in a substantial increase in the number of cavitation bubbles [34, 38], which can form a dense cloud of bubbles near the transducer which acts to block the energy transmitted from the transducer to the liquid [2, 17]. Also, an increase in the acoustic amplitude causes the generation of large numbers of bubbles, which may coalesce and escape before the collapse [17]. Thus, the net effect of all this could result in optimum acoustic amplitude giving a maximum sonochemical effect (see, e.g., Ref. [46]).

Additionally, with the increasing of the aqueous temperature, though the yield associated with the individual cavity decreases, the number of cavitation bubbles increases, though this results in a lowering of the cavitation threshold due to the rise in vapor pressure associated with heating of liquid [2]. The bubble–bubble coalescence may also be increased with the liquid temperature. Thus, the net effect of the bulk temperature increasing could result in an optimum reaction temperature for the maximum sonochemical efficiency (see, e.g., Ref. [43]).

In summary, despite all the considerations discussed above concerning the effects of operating parameters on the bubbles number and bubble–bubble interactions, the present theoretical simulations on the effects of acoustic amplitude, static pressure, and liquid temperature on single-bubble sonochemistry showed a good apparent trend between the model based on the single-bubble system and a substantial amount of experimental studies conducted in the field of sonochemistry. The model developed in this work, although simple, should practically aid in the optimization of the operating parameters in sonochemistry applications. The methodology adopted in this study is a useful starting point for the modeling and designing of sonochemical reactors.

Conclusion

Numerical simulations of chemical reactions inside an isolated spherical oxygen bubble have been performed at 300 kHz for different acoustic amplitudes, various static pressures, and diverse liquid temperatures, using a model that combines the dynamics of bubble collapse with the chemical kinetics of a single bubble of oxygen. The numerical simulations have revealed that $^{\bullet}OH$ radical and O atoms are the main oxidants created in the bubble. It was found that the amount of the oxidants created in the bubble increased as the acoustic amplitude increased. There exists an optimal static pressure for the production of the oxidants which depends on the acoustic amplitude. The optimal static pressure shifts toward a higher value as the acoustic amplitude increases. Correspondingly, an optimal liquid temperature (20 °C) has been observed for many oxidizing species ($^{\bullet}OH$, $HO_2^{\bullet}$ and H_2O_2), above which further increases cause a monotonically decrease in the production of the oxidants. At 1.5 and 2 atm, the amount of the oxidants presents a maximum at 20 °C. At 2.5 and 3 atm, there is no optimum, but the amount of the oxidants starts with a plateau at low temperatures (less than 15 °C) and then decreases sharply with further increases in liquid temperature above 15 °C. The simple model developed in

this work, after comparisons of the trends, seems to satisfactorily explain the experimental observations and should practically aid in optimization of the sonochemical operating conditions.

Acknowledgments The financial support by the General Directorate for Scientific Research and Technological Development (PNR Project No. 4/D/25) and the Ministry of Higher Education and Scientific Research of Algeria (Projects No. J0101120090018 and J0101120120098) is greatly acknowledged.

References

1. K.S. Suslick, Y. Didenko, M.M. Fang, T. Hyeon, K.J. Kolbeck, W.B. McNamara, M.M. Mdleleni, M.M. Wong, Philos. Trans. R. Soc. Lond. A **357**, 335 (1999)
2. L.H. Thompson, L.K. Doraiswamy, Ind. Eng. Chem. Res. **38**, 1215 (1999)
3. Y.G. Adewuyi, Ind. Eng. Chem. Res. **40**, 4681 (2001)
4. P. Riesz, D. Berdahl, C.L. Christman, Environ. Health Perspect. **64**, 233 (1985)
5. Y.G. Adewuyi, Environ. Sci. Technol. **39**, 3409 (2005)
6. KS. Suslick, in *Encyclopedia of Physical Science and Technology, 3rd edn*. ed. by R.A. Meyers (Academic, San Diego, 2001)
7. V. Kamath, A. Prosperetti, F.N. Egolfopoulos, J. Acoust. Soc. Am. **94**, 248 (1993)
8. D.V. Prasad Naidu, R. Rajan, R. Kumar, K.S. Gandhi, V.H. Arakeri, S. Chandrasekaran, Chem. Eng. Sci. **49**, 877 (1994)
9. C. Gong, D.P. Hart, J. Acoust. Soc. Am. **104**, 2675 (1998)
10. K. Yasui, T. Tuziuti, M. Sivakumar, Y. Iida, J. Chem. Phys. **122**, 224706 (2005)
11. A.J. Colussi, L.K. Weavers, M.R. Hoffmann, J. Phys. Chem. A **102**, 6927 (1998)
12. S. Sochard, A.M. Wilhelm, H. Delmas, Ultrason. Sonochem. **4**, 77 (1997)
13. K.S. Suslick, D.A. Hammerton, R.E. Cline, J. Am. Chem. Soc. **108**, 641 (1986)
14. L.A. Crum, J. Acoust. Soc. Am. **73**, 116 (1983)
15. J.B. Keller, M.J. Miksis, J. Acoust. Soc. Am. **68**, 628 (1980)
16. Y. Hao, A. Prosperetti, Phys. Fluids **11**, 2008 (1999)
17. N.P. Vichare, P. Senthilkumar, V.S. Moholkar, P.R. Gogate, A.B. Pandit, Ind. Eng. Chem. Res. **39**, 1480 (2000)
18. B.D. Storey, A.J. Szeri, Proc. R. Soc. Lond. A **456**, 1685 (2000)
19. S. Fujikawa, T. Akamatsu, J. Fluid Mech. **97**, 481 (1980)
20. RK. Sinnott, *Coulson & Richardson's Chemical Engineering, vol. 6, 4th edn*. (Elsevier Butterworth–Heinemann, Oxford, 2005), pp. 937–957
21. Coker AK, *Fortran programs for chemical process design, analysis, and simulation*. (Gulf Publishing Company, Houston, Texas, 1995), pp. 104–108
22. C.S. Dutcher, A.S. Wexler, S.L. Clegg, J. Phys. Chem. A **114**, 12216 (2000)
23. M. Laliberté, J. Chem. Eng. Data **52**, 321 (2007)
24. W. Wagner, H-J. Kretzschmar, *International steam tables: properties of water and steam based on the industrial formulation IAPWSIF97, 2nd edn* (Springer, Berlin, 2008), pp. 170–188
25. Beaton CF, Hewitt GF, Physical property data for the design engineer (Hemisphere, New York, 1989), pp. 273–306
26. M.O. Conaire, H.J. Curran, J.M. Simmie, W.J. Pitz, C.K. Westbrook, Int. J. Chem. Kinet. **36**, 603 (2004)
27. M.A. Mueller, T.J. Kim, R.A. Yetter, F.L. Dryer, Int. J. Chem. Kinet. **31**, 113 (1999)
28. B.-S. Choi, J.S. Oh, S.-W. Lee, H. Kim, J. Yi, Ind. Eng. Chem. Res. **40**, 4040 (2001)
29. M.A. Beckett, I. Hua, J. Phys. Chem. A **105**, 3796 (2001)
30. J.W. Kang, H.M. Hung, A. Lin, M.R. Hoffmann, Environ. Sci. Technol. **3**, 3199 (1993)
31. S. Koda, T. Kimura, T. Kondo, H. Mitome, Ultrason. Sonochem. **10**, 149 (2003)
32. A. Brotchie, F. Grieser, M. Ashokkumar, Phys. Rev. Lett. **102**, 084302 (2009)
33. B.P. Barber, C.C. Wu, R. Lofsted, P.H. Roberts, S.J. Putterman, Phys. Rev. Lett. **72**, 1380 (1994)
34. S, Labouret, J. Frohly, 10ème Congrès Français d'Acoustique (2010), http://hal.archives-ouvertes.fr/docs/00/55/11/51/PDF/000441.pdf

35. S. Merouani, O. Hamdaoui, Y. Rezgui, M. Guemini, Ultrason. Sonochem. **20**, 815 (2013)
36. S. Merouani, O. Hamdaoui, F. Saoudi, M. Chiha, J. Hazard. Mater. **178**, 1007 (2010)
37. G. Mark, A. Tauber, R. Laupert, H.-P. Schechmann, D. Schulz, A. Mues, C. Von Sonntag, Utrason. Sonochem. **5**, 41 (1998)
38. P. Kanthale, M. Ashokkumar, F. Grieser, Ultrason. Sonochem. **15**, 143 (2008)
39. R.A. Torres, C. Pétrier, E. Combet, M. Carrier, C. Pulgarin, Ultrason. Sonochem. **15**, 605 (2008)
40. A. Weissler, J. Acoust. Soc. Am. **24**, 651 (1953)
41. A. Henglein, A. Gutierrez, J. Phys. Chem. **97**, 158 (1993)
42. M.M. Van Iersel, J.-P.A.J. Den Manacker Van, N.E. Benes, J.T.F. Keurentjes, J. Phys. Chem. B **111**, 3081 (2007)
43. M.H. Entezari, P. Kruus, Utrason. Sonochem. **3**, 19 (1996)
44. T.J. Mason, J.P. Lorimer, D.M. Bates, Y. Zhao, Utrason. Sonochem. **1**, S91 (1994)
45. Y. Iida, K. Yasui, T. Tuziuti, M. Sivakumar, Microchem. J. **80**, 159 (2005)
46. M. Cutierrez, A. Henglein, J. Phys. Chem. **94**, 3625 (1990)